Test of charge-conjugation symmetry via microwave spectroscopy of positronium

R. J. Daly,[1] K. P. Habdas,[1] D. M. Newson,[1] J. Pérez-Ríos,[2] R. E. Sheldon,[1] and D. B. Cassidy[1]
[1]*Department of Physics and Astronomy, University College London, Gower Street, London WC1E 6BT, United Kingdom*
[2]*Department of Physics and Astronomy, Stony Brook University, Stony Brook, New York 11794, USA*

(Received 23 July 2025; accepted 30 October 2025; published 1 December 2025)

The $2\,^3S_1 \rightarrow 2\,^1P_1$ interval in positronium has been measured via microwave spectroscopy. This transition is strictly forbidden by charge conjugation invariance but may be observed in a magnetic field. Extrapolation of the Rabi frequencies obtained from spectral line shapes measured in different fields to the zero field case was used to test for a possible C-violating interaction with Hamiltonian H_{CV}, characterized by the matrix element $M_{\mathrm{CV}} = \langle 2\,^1P_1|H_{\mathrm{CV}}|2\,^3P_1\rangle$. We obtain $|M_{\mathrm{CV}}| = 18.6 \pm 6.5$ MHz and $|M_{\mathrm{CV}}| = 37.2 \pm 13.4$ MHz for the $M_J = \pm 1 \rightarrow \pm 1$ and the $M_J = 0 \rightarrow 0$ components, respectively.

DOI: 10.1103/trnb-hgr6

I. INTRODUCTION

Modern physics, as defined by the Standard Model (SM), is built upon symmetries [1]. Conserved quantities like energy and momentum can be directly linked to the symmetric nature of time and space [2], while fundamental interactions between particles may be described by various types of "internal" gauge symmetries [3]. There also exist discrete symmetries, which describe conserved properties related to noncontinuous changes, such as exchanging charges (C-symmetry), spatial inversion (parity, P), and time-reversal symmetry (T) [4]. If a system exhibits charge conjugation invariance, for example, then it will remain unchanged if the signs of all charges (or, more properly, all internal quantum numbers) are reversed. Similarly, parity transformations (i.e., inverting one or more spatial coordinates) leaves a system unchanged if P symmetry holds. Combinations of discrete symmetries, such as CP and CPT, are also observed to apply in many cases, and CPT symmetry in particular is thought to be inviolate in any Lorentz invariant quantum field theory [5].

These discrete symmetries were all once thought to rigorously apply to all fundamental interactions, but it was discovered that parity is in fact violated in weak interactions [6,7]. This was very surprising at the time and stimulated further investigations into other possible symmetry breaking scenarios; some of the observed P violation effects in weak interactions also demonstrate C violations [8,9]. T symmetry is difficult to test directly as there is no known mechanism for reversing time, but it can be probed indirectly [10,11]. CP violation is allowed in the SM and has been observed in the quark sector, initially in kaon decays [12] but later in many other systems (e.g., Refs. [13,14]). No CP violating processes have been unambiguously observed in the lepton sector, but the existence of mixing between different neutrino flavors is suggestive of such a mechanism [15]. This is of interest because leptogenesis is one possible explanation for the observed matter-antimatter asymmetry in the Universe [16,17].

There have been many recent tests of fundamental and "new" physics based on techniques developed for atomic and molecular physics, including experimental probes of symmetry violations and searches for dark matter, dark energy, and new particles and forces [18]. As a purely leptonic atom, positronium (Ps) [19] may be used to test discrete symmetries [20–24] as well as bound-state QED theory [25] via precision measurements of its energy levels, decay rates, or decay modes [26]. This is possible because, as a composite entity made up from a particle-antiparticle pair, Ps is an eigenstate of C, P, and CP, with eigenvalues of $(-1)^{L+S}$, $(-1)^{L+1}$, and $(-1)^{1+S}$, respectively [27], where L and S refer to the total Ps orbital angular momentum and spin quantum numbers, respectively. The C eigenvalue of a photon is (–1), and for N photons it is $(-1)^N$. Thus, if Ps annihilation is to conserve C symmetry, then the number of photons produced in Ps decay processes must be even (odd) for C-even (C-odd) eigenstates [28]. Hence, C invariance can be tested in experiments designed to observe the number of photons produced in individual Ps annihilation events [29–31].

Similarly, single-photon transitions between states with the same C eigenvalues also violate C-symmetry, and this allows for spectroscopy-based tests via direct searches for C-forbidden transitions [32]. Here we report such a test, conducted along the same lines as two previous experiments [33,34]. We consider single-photon transitions between the $2\,^3S_1$ and $2\,^1P_1$ levels of Ps. As both states have the same C eigenvalue (–1), direct single-photon transitions between them are C forbidden, as well as being forbidden by electric dipole selection rules [35]. Such transitions may occur; however, if the singlet and triplet P_1 levels are coupled by an interaction characterized by a Hamiltonian H_X, with the associated

Published by the American Physical Society under the terms of the Creative Commons Attribution 4.0 International license. Further distribution of this work must maintain attribution to the author(s) and the published article's title, journal citation, and DOI.

matrix element $M_X = \langle 2\,^1P_1|H_X|2\,^3P_1\rangle$. As described by Conti, Hatamian, and Rich [32], the transition amplitude in this case will be given by

$$A_X = \frac{\langle 2\,^1P_1|H_X|2\,^3P_1\rangle\langle 2\,^3P_1|E1|2\,^3S_1\rangle}{E_F}, \qquad (1)$$

where $E1$ indicates an electric dipole transition and E_F refers to the energy difference between the states coupled via H_X (i.e., $2\,^1P_1$ and $2\,^3P_1$) = 1.83 GHz [36]. The interaction coupling the P_1 levels could arise from an external magnetic field ($H_X = H_Z$) [37], or via some C-symmetry violating process ($H_X = H_{CV}$). This means that experiments can be conducted by measuring Zeeman-enabled transitions as a way to determine the system response, with tests for C-symmetry performed by extrapolating the strength of the resulting signal to the zero field case.

II. EXPERIMENTAL METHODS

The experimental methods used in this work are similar to those employed in previous microwave spectroscopy experiments [38–40] and are described in detail elsewhere [41,42]. We have, however, improved the waveguide design here and no longer observe any difference when the microwave radiation propagation direction is reversed [40]. In addition to changing the vacuum system to eliminate reflections [40], we (1) reduced a small (submillimeter) offset between the transmission grid and the internal surface of the waveguide and (2) checked and adjusted antenna installation using a vector network analyzer so as to match the signal transmission in each direction. Although we cannot be sure which of these modifications may have had the most impact, the fact that the signal was subsequently unchanged (within measurement errors) upon reversal of the microwave propagation direction indicates that, following the adjustments, the microwave fields in the guide were not significantly affected by reflections or other perturbing effects.

A pulsed positron beam, 3.5 ns wide (full width at half maximum) containing $\approx 10^5$ positrons was generated using a two-stage Surko-type buffer gas trap [43] operating at a 1 Hz repetition rate. This beam was implanted into a mesoporous silica film [44], and the resulting ground-state Ps atoms were optically driven to metastable $2\,^3S_1$ states using a Stark-mixing scheme [45]. The experiments were performed in an axial magnetic field whose strength could be varied from 70 to 150 G, which was measured with an accuracy of $\approx 1\%$.

Ps atoms excited to the $2\,^3S_1$ level passed through a high-transmission tungsten mesh into a WR-75 waveguide (i.e., with dimensions of 19.05×9.525 mm) where microwave transitions were driven, as indicated in Fig. 1. Using the measured mean Ps longitudinal velocity $v_z = 140$ km/s [46], the transit time of Ps atoms through the waveguide was found to be $T = 68$ ns. The waveguide was able to propagate TE_{10} mode radiation with frequencies in the range 10–15 GHz, suitable for driving both the $2\,^3S_1 \rightarrow 2\,^3P_1$ ($\nu_1 = 13012.41$ MHz) and $2\,^3S_1 \rightarrow 2\,^1P_1$ ($\nu_F = 11185.37$ MHz) transitions [26]. This made it possible to perform contemporaneous measurements of both transitions and hence to use ν_1 line shapes to characterize some waveguide properties relevant to the ν_F measurements.

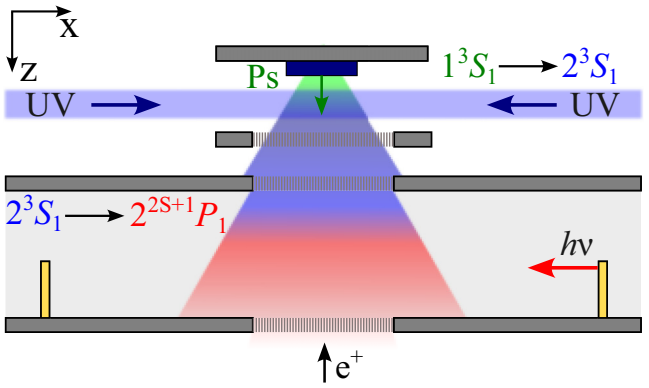


FIG. 1. Schematic representation of the experimental apparatus showing the Ps production target, the retro-reflected UV laser path, and the WR-75 waveguide in which $2\,^3S_1 \rightarrow 2\,^{2S+1}P_1$ ($S = 0, 1$) transitions are driven.

In order to connect the Rabi frequencies obtained from line-shape modeling (see Sec. IV) to the M_{CV} matrix elements [see Eq. (1)], it is necessary to know the amplitude of the oscillating electric field ($\mathcal{E}_0$) inside the waveguide. This can be done directly for ν_1 since, as discussed below, there is only one component to the transition. To determine this field we use the following procedure: The Rabi frequency for the ν_1 transition (Ω_1) was obtained from measured data (see Sec. V) recorded with $P_{\text{input}} = 40$ mW. The corresponding electric field amplitude was then determined using $\mathcal{E}_0(\nu_1) = \hbar\Omega/d_{2S_1,2P_1}$, where $d_{2S_1,2P_1} = 4.24ea_0$ is the electric dipole transition moment [38], e is the electronic charge, and a_0 is the Bohr radius. This yields $\mathcal{E}_0(\nu_1) = 4.3 \pm 0.1$ V/cm. The electric field in a waveguide depends on both the power (P_g) and frequency (ν) of the radiation according to $\mathcal{E}_0^2(\nu) \propto P_g[1 - \nu_c^2/\nu^2]^{-1/2}$ [47], where ν_c is the cut-off frequency of the waveguide (7.869 GHz for WR-75) [48]. Thus, for the ν_F measurements, where $P_{\text{input}} = 646$ mW, we obtain $\mathcal{E}_0(\nu_F) = 18.1 \pm 0.4$ V/cm. We cannot discount the possibility that there could be an additional frequency-dependent power coupling into the waveguide, so that the fraction of P_{input} contributing to P_g at the ν_F frequency might be different from the ν_1 case. To allow for this we assign a more conservative error of ± 3 V/cm. Hence, we obtain $\mathcal{E}_0(\nu_F) = 18 \pm 3$ V/cm.

Spectral line shapes were measured via a single-shot lifetime method [49] using a set of four LYSO based γ-ray detectors [50]. Driving transitions from long-lived $2\,^3S_1$ levels to any of the $2P$ states significantly increases the Ps decay rate. Thus, the effect of microwave radiation was characterized by the parameter $S_\gamma(\nu)$, which is proportional to the fraction of $2\,^3S_1$ atoms that undergo microwave-induced transitions, and which was obtained from lifetime spectra recorded with and without microwave radiation present (see Ref. [41] for details). Example line shapes of ν_1 and ν_F transitions are shown in Fig. 2.

III. ZEEMAN MIXING

The methodology used in the experiments we report is based on the fact that, by performing measurements in a magnetic field, we can observe an analog of the C-forbidden

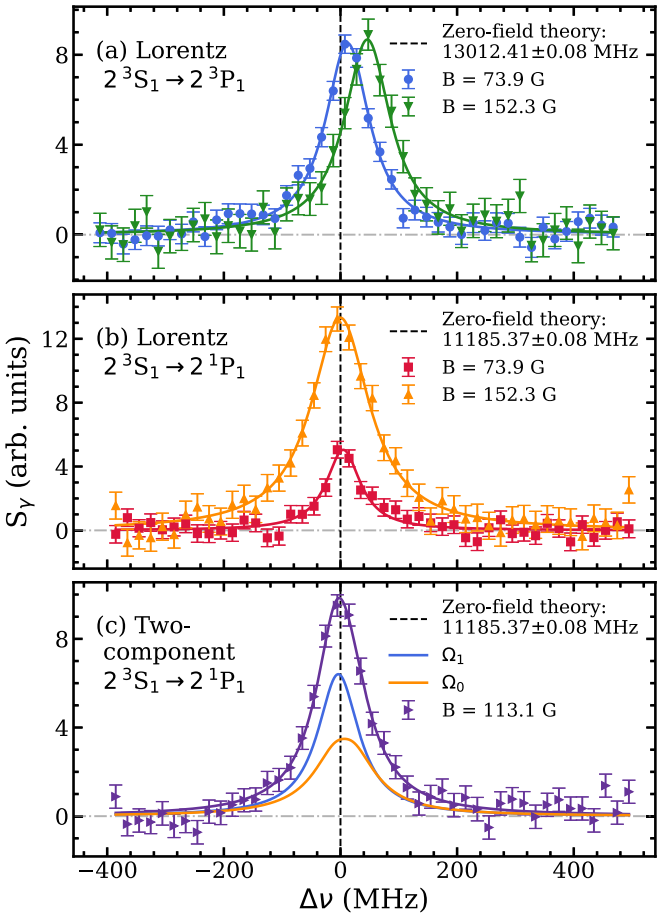


FIG. 2. Measured line shapes for ν_1 (a) and ν_F (b) transitions in magnetic fields of strength 73.9 G and 152.3 G, as indicated in the legends. The solid lines in (a) and (b) are Lorentzian fits. The data in (c) were recorded in a magnetic field of 113.1 G, and the solid line is a two-component fit made using the line-shape function Eq. (4), with the two components explicitly shown. In all panels the vertical dashed lines indicate the relevant theoretical zero-field transition frequency.

ν_F transition, and then by extrapolation to zero field we may test for any residual signal, which would then be associated with a C-violating interaction characterized by the matrix element $M_{\rm CV}$ as described above. Thus, the experiments are necessarily conducted in a magnetic field, which mixes singlet and triplet levels, and the ν_F transition comprises two Zeeman shifted components, as indicated in Fig. 3. Since the orientation of the microwave guide is such that the RF field is linearly polarized along the direction of the magnetic field, only transitions for which $\Delta M_J = 0$ are driven [38]. This means that the $2\,^3S_1 \to 2\,^1P_1$ transition occurs in two different flavors, $M_J = 0 \to 0$, and $M_J = \pm 1 \to \pm 1$, where the former only occurs via $2\,^3P_2/2\,^1P_1$, mixing, and the latter through both $2\,^3P_2/2\,^1P_1$ and $2\,^3P_1/2\,^1P_1$ mixing. We neglect effects from the much weaker contribution from $2\,^3P_0/2\,^1P_1$ mixing.

The associated mixing coefficients $|A_{JM_J}|$ and corresponding Zeeman shifts for these transitions are shown in Fig. 4. These coefficients represent the admixture between $2\,^3P_J$ and $2\,^1P_1$ for a given M_J value and are obtained from diagonaliza-

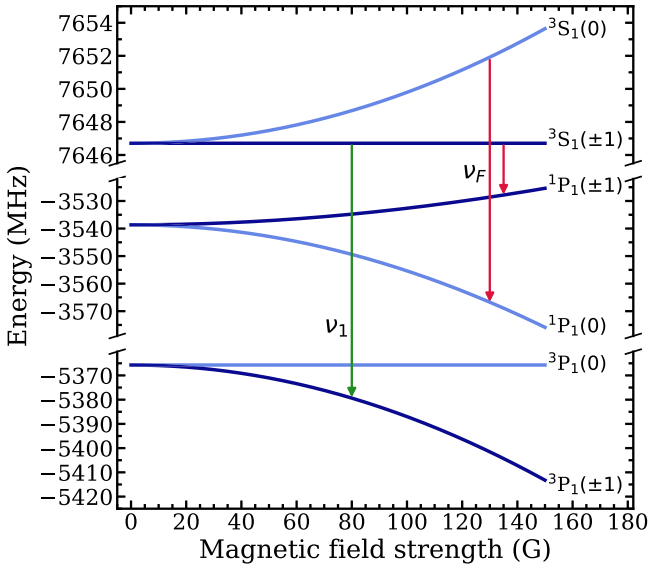


FIG. 3. Zeeman structure of Ps levels, relative to the $(n = 2)$ Bohr level. The green (red) arrows represent the allowed transitions constituting the ν_1 (ν_F) transitions for which $\Delta M_J = 0$.

tion of the Ps Zeeman Hamiltonian [51,52]. The ν_1 transition comprises only a single component that is shifted to higher frequencies in the magnetic field, as can be directly observed in the line shapes shown in Fig. 2(a). The ν_F transition contains components that exhibit both positive and negative Zeeman shifts; the weighted average, taking into account the

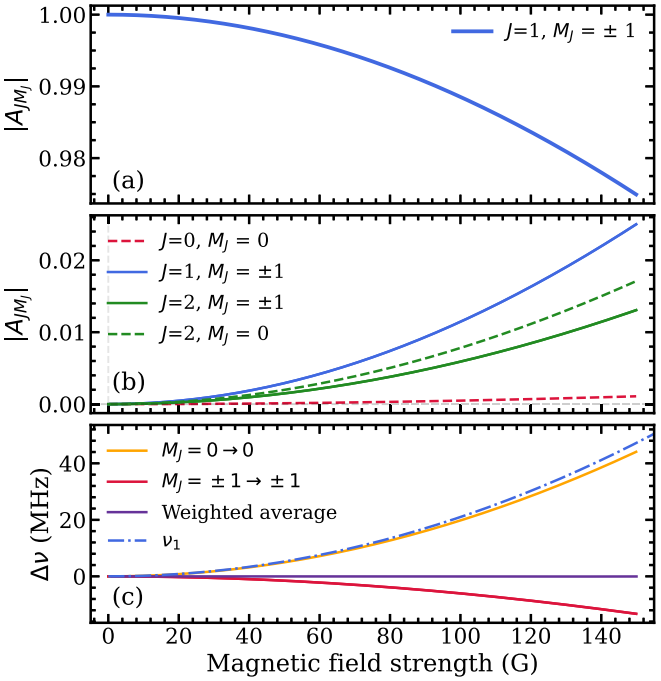


FIG. 4. Zeeman-mixing coefficients, $|A_{JM_J}|$ for the ν_1 (a) and ν_F (b) transitions, as described in the text. The corresponding Zeeman shifts are shown in (c), including the weighted average for the ν_F transition, obtained using the relative transition strengths and angular integrals.

number of substates and their transition strengths, is relatively flat, as indicated in Fig. 4(c).

IV. LINE-SHAPE MODEL

In some previous experiments asymmetric line shapes were observed [38] that had to be modeled using empirical asymmetric line functions or a more complicated Monte Carlo approach [53]. These effects were eliminated using an improved apparatus with fewer reflections, allowing us to use symmetric Lorentzian functions to fit line shapes. However, although Lorentzian functions are sufficient for fitting symmetric line shapes [38] and extracting linewidths and centroid frequencies [54], a more detailed line-shape model is required to determine the Rabi frequencies of the underlying transitions. We apply a model developed for hydrogen (see, e.g., Ref. [55] for details) to the Ps system. We approximate Ps as a two-level system, labeling the final ($2\,^3P_1$) and initial ($2\,^3S_1$) states with the $|f\rangle$ and $|i\rangle$ kets, respectively, and adopt the ansatz $|\Psi(t)\rangle = c_f(t)|f\rangle + c_i(t)e^{-\imath\omega_{fi}t}|i\rangle$, where ω_{fi} denotes the frequency difference between the two states under consideration. The time-dependent Schrödinger equation yields

$$\dot{c}_f(t) = \frac{\imath\Omega}{2}c_i(t)e^{-\imath\tilde{\Delta}t}, \quad \dot{c}_i(t) = \frac{\imath\Omega}{2}c_f(t)e^{\imath\tilde{\Delta}t}, \tag{2}$$

where the detuning is defined as $\tilde{\Delta} \to \Delta + \imath\gamma_f/2$ including the natural decay width of the final state via spontaneous emission, denoted by γ_f, Δ is the detuning of the microwave frequency with respect to the relevant atomic transition, and $\Omega = \langle f|d|i\rangle\mathcal{E}_0/\hbar$ is the corresponding Rabi frequency. This transformation is equivalent to solving the damped Bloch equations for a two-level atom [56,57]. For the sake of simplicity, we assume $\gamma_f = \gamma = 2\pi \times 50$ MHz and $\gamma_i = 0$. We employ the method of Rabi [55] to solve Eqs. (2), yielding $c_i(t) = Ae^{\imath\mu_+ t} + Be^{\imath\mu_- t}$, where $\mu_\pm = \frac{\Delta+\imath\gamma/2}{2} \pm \frac{\lambda}{2}$ and $\lambda = \sqrt{(\Delta+\imath\gamma/2)^2 + \Omega^2}$. Next, imposing the initial conditions: $c_i(0) = 1$ and $c_f(0) = 0$, the line shape, or the absorption probability is given by $1 - |c_i(t)|^2$, representing the probability of finding the atom in the ground state given an interaction time T with the radiation (68 ns), yielding

$$\mathcal{L}(A,\Omega,\Delta,\gamma,T) = A\left(1 - e^{-\frac{\gamma}{2}T}\left|\cos\left(\sqrt{(\Delta+\imath\gamma/2)^2+\Omega^2}T/2\right) + \frac{(-\imath\Delta+\gamma/2)\sin\left(\sqrt{(\Delta+\imath\gamma/2)^2+\Omega^2}T/2\right)}{\sqrt{(\Delta+\imath\gamma/2)^2+\Omega^2}}\right|^2\right), \tag{3}$$

where A is a scaling factor connecting the signal amplitude to the measured S_γ values. Examples of single-component fits to ν_F data using Eq. (3) are shown in Fig. 2(b). This line-shape model applies to only one of the Zeeman components. However, since the ν_F transition actually comprises two components, with different Zeeman shifts, the complete ν_F line shape is given by

$$\mathcal{L}(\Delta_{\pm1},\Delta_0,\gamma,T,B) = \tfrac{1}{3}[2L(\Omega_{\pm1}(B),\Delta_{\pm1},\gamma,T) + L(\Omega_0(B),\Delta_0,\gamma,T)], \tag{4}$$

where $\Delta_{\pm1}$ and Δ_0 represent the detuning for the same microwave frequency from different centroids associated with the $M_J = \pm1 \to \pm1$ and $M_J = 0 \to 0$ transitions, respectively. Ω_{JM_J} represents the Rabi frequency for $2\,^1P_{JM_J}$ to $2\,^3S_{1M_J}$ transitions. The factor of $1/3$ accounts for all contributing transitions. An example of a fit to ν_F data using Eq. (4) is shown in Fig. 2(c), including the contributions from different components.

V. RESULTS

As shown in Fig. 4, the different Zeeman components are shifted by much less than the observed linewidths (≈100 MHz) in the range of magnetic fields studied, and therefore they cannot be explicitly resolved. Because of this it is necessary to fit a two-component function [Eq. (4)] to obtain individual Rabi frequencies. The Rabi frequencies obtained from the two-component fits as a function of the magnetic field are shown in Fig. 5. In the absence of a C-violating interaction, all ν_F Rabi frequencies should go to zero with the magnetic field. For comparison we also show in Fig. 5 the ν_1 Rabi frequencies, obtained using Eq. (3); as expected, these do not depend on the magnetic field. The average value of the ν_1 Rabi frequencies obtained was 17.72 ± 0.33 MHz. As described in Sec. II, these data were used to determine the electric field amplitude in the waveguide.

The measured Rabi frequencies, Ω_{JM_J} for a given $2\,^1P_{JM_J}$ component fulfill

$$\Omega^2_{JM_J}(B,I) = 288\pi\alpha a_0^2 I C_{JM_J} A_{JM_J}(B)/\hbar^2, \tag{5}$$

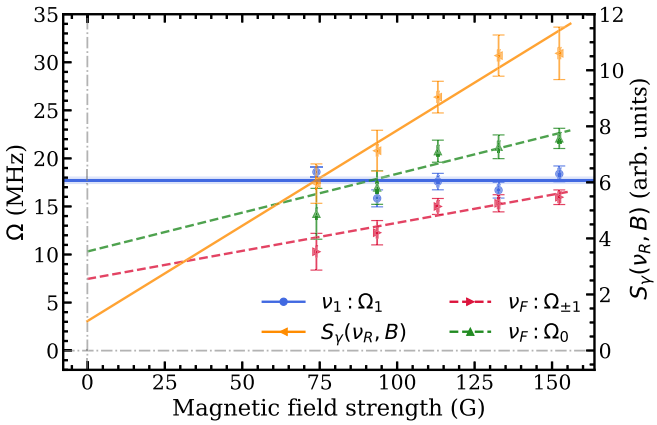


FIG. 5. Rabi frequencies for ν_1 and ν_F extracted from the line-shape fitting described in the text, over a range of magnetic fields. The average value of the ν_1 Rabi frequencies (17.72 ± 0.33 MHz) is indicated by the horizontal blue line. Linear fits (dashed lines) were applied to the various components of the ν_F data as indicated in the legend, and extrapolated to zero field. The obtained values are shown in Table I. Also shown are line-shape amplitudes $S_\gamma(\nu_R, B)$ obtained from Lorentz fits to data from one of the detectors used, from which we obtain $S_\gamma(\nu_R, 0) = 1.05 \pm 1.43$. An error of ±1 G has been applied to the magnetic field values.

TABLE I. Zero-field ν_F Rabi frequencies obtained from the data in Fig. 5 and corresponding values of $|M_{\rm CV}|$ obtained from Eq. (7). Also shown are the 1 σ (i.e., one standard deviation) errors of the $|M_{\rm CV}|$ values.

M_J	$\Omega_{M_J}(0)$ (MHz)	$\lvert M_{\rm CV}\rvert$ (MHz)	σ
1	7.46 ± 2.38	18.6 ± 6.5	2.9
0	10.31 ± 3.30	37.2 ± 13.4	2.8

where I is the intensity of the rf field, α is the fine structure constant, a_0 is the Bohr radius, and C_{JM_J} is an angular factor related to the Clebsch-Gordan coefficients: $C_{10} = 0$, $C_{1\pm1} = 1/2$, $C_{2\pm1} = 1/2$, and $C_{20} = 2/3$. From the multicomponent fitting approach we obtain $\Omega_{M_J}(B)$ (see Fig. 5). At zero magnetic field, and in the presence of a charge-violating interaction, we would expect a residual Rabi frequency corresponding to the transition amplitude in Eq. (1). The result is a pure charge-violation amplitude, $|M_{\rm CV}| = |\langle 2\,^1P_1|H_X|2\,^3P_J\rangle|$, i.e., we assume that $|M_{\rm CV}|$ is the same for any J transition, weighted by the $E1$ contribution

$$|\langle 2\,^3P_J|E1|2\,^3S_1\rangle| = 6ea_0\mathcal{E}_0\sqrt{C_{JM_J}}. \tag{6}$$

Hence, only $M_J = \pm1 \to \pm1$ and the $M_J = 0 \to 0$ transitions are relevant, so we average over J. Then we find

$$\Omega_{M_J}(0) = \frac{(6ea_0)\mathcal{E}_0}{\hbar}|M_{\rm CV}|\sqrt{\sum_J \frac{C_{JM_J}}{E_J^2}}, \tag{7}$$

where E_J is the energy difference between the $2\,^1P_1$ and the corresponding $2\,^3P_J$ level. The $|M_{\rm CV}|$ values obtained from the different $\Omega_{M_J}(0)$ data are summarized in Table I.

The strength of the ν_F signal can also be described qualitatively via the signal amplitude on resonance $S_\gamma(\nu_R, B)$. Figure 5 also shows this amplitude, obtained from Lorentz fitting, and this is consistent with zero in zero field ($S_\gamma(\nu_R, 0) = 1.05 \pm 1.43$). However, this approach does not provide a direct value of $|M_{\rm CV}|$.

VI. DISCUSSION AND CONCLUSIONS

The $|M_{\rm CV}|$ results obtained are shown in Table I. These data are ostensibly consistent with a C-violation process, but only at the level of $\approx 3\sigma$. It is evident from the data shown in Fig. 5 that, although we do observe a linear dependence on B, our obtained Rabi frequencies, and hence $|M_{\rm CV}|$ values, do not tend towards zero at zero field, even though the signal parameter $S_\gamma(\nu_R, 0)$ does. This indicates that the two-component fitting procedure is not able to accurately extract the unresolved components. In principle a more detailed line-shape model could be employed that included relevant effects explicitly (such as Stark shifts or line broadening mechanisms), but since the underlying components are not resolved this would be unlikely to provide any further advantage.

One way to address this problem would be to irradiate the incident $2\,^3S_1$ beam with high-power microwave radiation at $\approx$18.5 GHz to drive $2\,^3S_1 \to 2\,^3P_0$ transitions [38]. This would depopulate the $M_J = 0$ sublevel, so that the subsequent ν_F transitions would contain only the $M_J = \pm1 \to \pm1$ components. Alternatively, if higher magnetic fields (on the order of 300–500 G) were used, then both underlying components could be sufficiently Zeeman shifted to be separately resolved, also allowing for direct extrapolation to zero field for each component.

Despite these limitations, the measurement we describe here may be compared with previous C-symmetry tests using the ν_F transition, which found $|M_{\rm CV}| < 64$ MHz [33] and $|M_{\rm CV}| < 76$ MHz [34]. The measurement we report here is slightly different in character to these as our methodology provides a specific value for $|M_{\rm CV}|$ rather than an upper limit. As described by Conti *et al.*, the ratio $\eta_{\rm CV} = |M_{\rm CV}|/E_F$ [cf. Eq. (1)] may be interpreted as a measure of the amount of CP mixing (with C violation, and P conserved) between the $2\,^1P_1$ and $2\,^3P_J$ levels [33]. Using the Ω_1 component we obtain $|M_{\rm CV}| = 18.6 \pm 6.5$ MHz, and thus $\eta_{\rm CV} = (10.2 \pm 3.6) \times 10^{-3}$. This mixing fraction can be compared with (indirect) CP violation in mesons, arising from mixing CP even and odd states, that may be observed via CP violating decays (e.g., Ref. [58]). Specifically, in neutral kaon decays the mixing state $|\epsilon| = |A(K_L \to \pi\pi)|/|A(K_S \to \pi\pi)| = (2.228 \pm 0.011) \times 10^{-3}$, where $K_L(K_S)$ represent the kaon long (short) lived $K_0, \bar{K}_0$ composite states [59].

It should be understood that the comparison between our measurement of possible C violation in Ps transitions, and that of (indirect) CP violation in neutral kaon decays does not represent a complementary test of a single underlying symmetry violating interaction. Indeed, CP violation in the quark sector at this level can be fully accommodated in the SM, whereas the Ps measurements test only electromagnetic interactions or some kind of new physics, and hence any verified signal would represent a significant departure from currently accepted SM physics. Rather, the comparison of $\eta_{\rm CV}$ with $|\epsilon|$ indicates the relative sensitivity with which the different experiments probe these effects. Thus, in this case the Ps measurement is approximately a factor of 5 less sensitive than the kaon decay measurements.

By implementing experimental modifications that would make it possible to resolve the Zeeman shifted components we expect to improve the experiments and exceed the sensitivity of the kaon measurements.

ACKNOWLEDGMENTS

We are grateful to S. D. Hogan, R. Pohl, and H. Metcalf for helpful comments and discussions, L. Liszkay for providing silica samples, and J. Dumper, F. Noyes, and R. Jawad for technical assistance. This work was supported in part by the UK Engineering and Physical Sciences Research Council (EPSRC) under Grant No. EP/W032023/1 and by the Simons Foundation.

DATA AVAILABILITY

The data that support the findings of this article are not publicly available. The data are available from the authors upon reasonable request.

[1] S. T. Love, The role of symmetry in the development of the standard model, in *Elements in Physics beyond the Standard Model with Atomic and Molecular Systems* (Cambridge University Press, Cambridge, UK, 2024).

[2] E. Noether, Invariante variationsprobleme, Nachrichten von der Gesellschaft der Wissenschaften zu Göttingen, Math.-Phys. Kl. **1918**, 235 (1918).

[3] D. Griffiths, *Introduction to Elementary Particles* (John Wiley & Sons, New York, 1987).

[4] M. Sozzi, *Discrete Symmetries and CP Violation: From Experiment to Theory* (Oxford University Press, Oxford, 2007).

[5] G. Lüders, Proof of the TCP theorem, Ann. Phys. **2**, 1 (1957).

[6] T. D. Lee and C. N. Yang, Question of parity conservation in weak interactions, Phys. Rev. **104**, 254 (1956).

[7] C. S. Wu, E. Ambler, R. W. Hayward, D. D. Hoppes, and R. P. Hudson, Experimental test of parity conservation in beta decay, Phys. Rev. **105**, 1413 (1957).

[8] J. I. Friedman and V. L. Telegdi, Nuclear emulsion evidence for parity nonconservation in the decay chain $\pi^+ - \mu^+ - e^+$, Phys. Rev. **105**, 1681 (1957).

[9] R. L. Garwin, L. M. Lederman, and M. Weinrich, Observations of the failure of conservation of parity and charge conjugation in meson decays: The magnetic moment of the free muon, Phys. Rev. **105**, 1415 (1957).

[10] R. R. Lewis, Time-reversal invariance in beta decay, Phys. Rev. **108**, 904 (1957).

[11] L. Caldwell, T. S. Roussy, T. Wright, W. B. Cairncross, Y. Shagam, K. Boon Ng, N. Schlossberger, S. Y. Park, A. Wang, J. Ye, and E. A. Cornell, Systematic and statistical uncertainty evaluation of the HfF^+ electron electric dipole moment experiment, Phys. Rev. A **108**, 012804 (2023).

[12] J. H. Christenson, J. W. Cronin, V. L. Fitch, and R. Turlay, Evidence for the 2π decay of the k_2^0 meson, Phys. Rev. Lett. **13**, 138 (1964).

[13] R. Aaij *et al.* (LHCb Collaboration), Observation of *CP* violation in charm decays, Phys. Rev. Lett. **122**, 211803 (2019).

[14] R. Aaij *et al.* (LHCb Collaboration), Observation of several sources of *CP* violation in $B^+ \to \pi^+\pi^+\pi^-$ decays, Phys. Rev. Lett. **124**, 031801 (2020).

[15] K. Abe *et al.* (The T2K Collaboration), Constraint on the matter-antimatter symmetry-violating phase in neutrino oscillations, Nature (London) **580**, 339 (2020).

[16] G. C. Branco, R. González Felipe, and F. R. Joaquim, Leptonic *CP* violation, Rev. Mod. Phys. **84**, 515 (2012).

[17] C. Hagedorn, R. N. Mohapatra, E. Molinaro, C. C. Nishi, and S. T. Petcov, *CP* violation in the lepton sector and implications for leptogenesis, Int. J. Mod. Phys. A **33**, 1842006 (2018).

[18] M. S. Safronova, D. Budker, D. DeMille, D. F. Jackson Kimball, A. Derevianko, and C. W. Clark, Search for new physics with atoms and molecules, Rev. Mod. Phys. **90**, 025008 (2018).

[19] J. A. Wheeler, Polyelectrons, Ann. N.Y. Acad. Sci. **48**, 219 (1946).

[20] W. Bernreuther, U. Löw, J. P. Ma, and O. Nachtmann, How to test *CP*, *T*, and *CPT* invariance in the three photon decay of polarized $^3S_1$ positronium, Z. Phys. C **41**, 143 (1988).

[21] M. Skalsey and J. Van House, First test of *CP* invariance in the decay of positronium, Phys. Rev. Lett. **67**, 1993 (1991).

[22] T. Yamazaki, T. Namba, S. Asai, and T. Kobayashi, Search for *CP* violation in positronium decay, Phys. Rev. Lett. **104**, 083401 (2010).

[23] B. K. Arbic, S. Hatamian, M. Skalsey, J. Van House, and W. Zheng, Angular-correlation test of *CPT* in polarized positronium, Phys. Rev. A **37**, 3189 (1988).

[24] P. A. Vetter and S. J. Freedman, Search for *CPT*-Odd decays of positronium, Phys. Rev. Lett. **91**, 263401 (2003).

[25] S. G Karshenboim, Precision study of positronium: Testing bound state QED theory, Int. J. Mod. Phys. A **19**, 3879 (2004).

[26] G. S. Adkins, D. B. Cassidy, and J. Pérez-Ríos, Precision spectroscopy of positronium: Testing bound-state QED theory and the search for physics beyond the standard model, Phys. Rep. **975**, 1 (2022).

[27] W. Bernreuther and O. Nachtmann, Weak interaction effects in positronium, Z. Phys. C **11**, 235 (1981).

[28] L. Wolfenstein and D. G. Ravenhall, Some consequences of invariance under charge conjugation, Phys. Rev. **88**, 279 (1952).

[29] A. P. Mills Jr. and S. Berko, Search for *C* nonconservation in electron-positron annihilation, Phys. Rev. Lett. **18**, 420 (1967).

[30] K. Marko and A. Rich, Search for orthopositronium decay into four photons as a test of charge-conjugation invariance, Phys. Rev. Lett. **33**, 980 (1974).

[31] J. Yang, M. Chiba, R. Hamatsu, T. Hirose, T. Matsumoto, and J. Yu, Four-photon decay of orthopositronium: A test of charge-conjugation invariance, Phys. Rev. A **54**, 1952 (1996).

[32] R. S. Conti, S. Hatamian, and A. Rich, Tests of the discrete symmetries *C*, *P*, and *T* in one-photon transitions of positronium, Phys. Rev. A **33**, 3495 (1986).

[33] R. S. Conti, S. Hatamian, L. Lapidus, A. Rich, and M. Skalsey, Search for C-violating, *P*-conserving interactions and observation of $2^3S_1 \to 2^1P_1$ transitions in positronium, Phys. Lett. A **177**, 43 (1993).

[34] R. Ley, D. Hagena, D. Weil, G. Werth, W. Arnold, and H. Schneider, Spectroscopy of excited state positronium, Hyperfine Interact. **89**, 327 (1994).

[35] W. Demtröder, *Laser Spectroscopy*, 3rd ed. (Springer, New York, 2003).

[36] A. Czarnecki, K. Melnikov, and A. Yelkhovsky, Positronium *S*-state spectrum: Analytic results at $O(m\alpha^6)$, Phys. Rev. A **59**, 4316 (1999).

[37] A. M. Alonso, B. S. Cooper, A. Deller, S. D. Hogan, and D. B. Cassidy, Positronium decay from $n = 2$ states in electric and magnetic fields, Phys. Rev. A **93**, 012506 (2016).

[38] L. Gurung, T. J. Babij, J. Pérez-Ríos, S. D. Hogan, and D. B. Cassidy, Observation of asymmetric line shapes in precision microwave spectroscopy of the positronium $2^3S_1 \to 2^3P_J (J = 1, 2)$ fine-structure intervals, Phys. Rev. A **103**, 042805 (2021).

[39] R. E. Sheldon, T. J. Babij, S. H. Reeder, S. D. Hogan, and D. B. Cassidy, Microwave spectroscopy of positronium atoms in free space, Phys. Rev. A **107**, 042810 (2023).

[40] R. E. Sheldon, T. J. Babij, S. H. Reeder, S. D. Hogan, and D. B. Cassidy, Precision microwave spectroscopy of the positronium $2^3S_1 \to 2^3P_2$ interval, Phys. Rev. Lett. **131**, 043001 (2023).

[41] B. S. Cooper, A. M. Alonso, A. Deller, T. E. Wall, and D. B. Cassidy, A trap-based pulsed positron beam optimised for positronium laser spectroscopy, Rev. Sci. Instrum. **86**, 103101 (2015).

[42] D. B. Cassidy, Experimental progress in positronium laser physics, Eur. Phys. J. D **72**, 53 (2018).

[43] J. R. Danielson, D. H. E. Dubin, R. G. Greaves, and C. M. Surko, Plasma and trap-based techniques for science with positrons, Rev. Mod. Phys. **87**, 247 (2015).

[44] L. Liszkay, C. Corbel, P. Perez, P. Desgardin, M. F. Barthe, T. Ohdaira, R. Suzuki, P. Crivelli, U. Gendotti, A. Rubbia, M. Etienne, and A. Walcarius, Positronium reemission yield from mesostructured silica films, Appl. Phys. Lett. **92**, 063114 (2008).

[45] A. M. Alonso, S. D. Hogan, and D. B. Cassidy, Production of 2^3S_1 positronium atoms by single-photon excitation in an electric field, Phys. Rev. A **95**, 033408 (2017).

[46] R. J. Daly, R. E. Sheldon, and D. B. Cassidy, Measurement of the fluorescence decay rate of 2^3P_J positronium, Phys. Rev. A **110**, 022807 (2024).

[47] D. Hagena, R. Ley, D. Weil, G. Werth, W. Arnold, and H. Schneider, Precise measurement of $n = 2$ positronium fine-structure intervals, Phys. Rev. Lett. **71**, 2887 (1993).

[48] N. Marcuvitz, *Waveguide Handbook* (The Institution of Engineering and Technology, London, 1986).

[49] D. B. Cassidy, S. H. M. Deng, H. K. M. Tanaka, and A. P. Mills Jr., Single shot positron annihilation lifetime spectroscopy, Appl. Phys. Lett. **88**, 194105 (2006).

[50] A. M. Alonso, B. S. Cooper, A. Deller, and D. B. Cassidy, Single-shot positron annihilation lifetime spectroscopy with LYSO scintillators, Nucl. Instrum. Methods A **828**, 163 (2016).

[51] S. M. Curry, Combined Zeeman and motional Stark effects in the first excited state of positronium, Phys. Rev. A **7**, 447 (1973).

[52] C. D. Dermer and J. C. Weisheit, Perturbative analysis of simultaneous Stark and Zeeman effects on $n = 1 \rightarrow n = 2$ radiative transitions in positronium, Phys. Rev. A **40**, 5526 (1989).

[53] L. A. Akopyan, T. J. Babij, K. Lakhmanskiy, D. B. Cassidy, and A. Matveev, Line-shape modeling in microwave spectroscopy of the positronium $n = 2$ fine-structure intervals, Phys. Rev. A **104**, 062810 (2021).

[54] L. Gurung, T. J. Babij, S. D. Hogan, and D. B. Cassidy, Precision microwave spectroscopy of the positronium $n = 2$ fine structure, Phys. Rev. Lett. **125**, 073002 (2020).

[55] M. Sargent, M. O. Scully, and W. E. Lamb, *Laser Physics* (Addison-Wesley, Reading, MA, 1974), Chap. xxvii.

[56] M. P. Sharma, D. A. Cardimona, and A. Gavrielides, Decay of a two-level atom, Phys. Rev. A **41**, 5237 (1990).

[57] J. R. Ackerhalt, Resonant pulse excitation leading to ionization, Phys. Rev. A **17**, 293 (1978).

[58] A. L. Kagan and M. D. Sokoloff, Indirect *CP* violation and implications for $D^0 - \overline{d}^0$ and $B_s - \overline{b}_s$ mixing, Phys. Rev. D **80**, 076008 (2009).

[59] S. Navas *et al.* (Particle Data Group), Review of particle physics, Phys. Rev. D **110**, 030001 (2024).